



Resistance Control of an Additively Manufactured Conductive Layer in Roll-to-Roll Gravure Printing Systems

Minho Jo¹ · Jongsu Lee² · Seongyong Kim¹ · Gyoujin Cho³ · Taik-Min Lee⁴ · Changwoo Lee⁵ 

Received: 23 December 2020 / Revised: 12 March 2021 / Accepted: 18 March 2021 / Published online: 8 April 2021
© Korean Society for Precision Engineering 2021

Abstract

Flexible pressure sensors, which are employed in robotic arms and electronic skin, are conventionally prepared using methods such three-dimensional printing, laser scribing, and spray coating. However, they are time-consuming and unsuitable for large-scale production. Thus, to overcome these limitations, roll-to-roll (R2R)-based fabrication techniques have been employed for low-cost mass production of flexible pressure sensors. Gravure printing is a promising R2R based technique, but it faces limitations in terms of ink-flow and printing defects causing short circuit, which may affect the performance of printed electronic devices. In this study, we analyzed the effects of printing conditions, web speed, tension, and nip pressure on the drag-out tail defects and conductance in the gravure printing process. We statistically optimized the optimal conditions to obtain minimum drag-out tail defects and conductance using a Box–Behnken design. We also fabricated two flexible pressure capacitive sensors using the conductive patterns to verify optimal conditions. Our results showed that the resistance decreased with increasing web speed, tension, and nip pressure, whereas the drag-out tail increased with increasing tension and nip pressure and decreasing web speed. Additionally, under the optimal conditions, the resistance and drag-out tail severity were improved by 74% and 53%, respectively, over those of the conventionally printed pattern. Finally, using the two flexible pressure capacitive sensors, we showed that the sensor using the conductive pattern had a higher sensitivity after optimization.

Keywords Additively manufactured conductive layer · Electrical performance · Optimization · Resistance control · Roll-to-roll gravure printing · Drag-out tail defect

1 Introduction

Roll-to-Roll (R2R) manufacturing processes have become a subject of interest because of their simplicity, low cost, and mass production. Because of these advantages, large-area flexible electronic devices, such as photovoltaics, fuel cells, and flexible sensors, have been fabricated using the R2R process [1, 2]. Notably, flexible pressure sensors can be used in robot arms and electronic skin [3–10]. To date, pressure sensors have been fabricated using three-dimensional printing, laser scribing, and spray coating [6, 11, 12]. These patterning methods are not adequate for the mass production of sensors and have low productivity and high production cost. Therefore, the R2R-based fabrication technique is essential for the low-cost and mass production of flexible pressure sensors. Gravure printing is a good candidate for making conductive patterns in the R2R process because of the long life of its printing roll and its high compatibility with the R2R process [13]. However, the behavior of ink in

✉ Changwoo Lee
changwoo1220@gmail.com

¹ Department of Mechanical Design and Production Engineering, Konkuk University, 120, Neungdong-ro, Gwangjin-gu, Seoul 05023, South Korea
² Department of Printed Electronics Engineering, Suncheon National University, 225, Jungang-ro, Suncheon 57922, South Korea
³ Institute of Quantum Biophysics, Sungkyukwan University, 2066 Seobu-ro, Jangan-gu, Suwon 16419, South Korea
⁴ Korea Institute of Machinery and Materials (KIMM), Intelligence and Precision Machinery Research Division, 156 Gajeongbuk-ro, Yuseong-gu, Daejeon 34103, South Korea
⁵ Department of Mechanical Engineering, Konkuk University, 120, Neungdong-ro, Gwangjin-gu, Seoul 05023, South Korea

the printing phase is more complex than that of inkjet printing, spray, and slot-die coating, and several printing factors such as web speed and nip pressure have a major interactive effect on the printing quality, which significantly affects the performance of electronic devices such as thin film transistors and flexible capacitors [14–16]. Several research groups have attempted to improve printing quality and resolution. Nguyen et al. analyzed the effect of the tension on the surface characteristics of the web and evaluated the printed pattern quality using the thickness and surface roughness of the pattern [17]. Lee et al. proposed a theoretical model that could express the effect of the shear force in the transferred ink from an engraved cell to substrate and pattern angle on the volume of the printed pattern [18]. Lee et al. developed a meta model to determine the variation in the surface roughness according to the tension disturbance [19]. Kang et al. developed a method to optimize the tension in a R2R process considering the change in the elastic modulus of the plastic film and conductance of the printed pattern in a dryer [20].

As mentioned above, most previous studies have focused on the ink transfer mechanism in gravure printing and the volume of printed pattern, thickness, and surface roughness according to the printing conditions. Considering the severity of printing defects that can generate a short circuit and the conductance simultaneously is very important. The most representative defect that can lead to a short circuit is caused by the relative motion between the engraved cell and tip of the doctor blade [21]. The drag-out tail area is very thin compared to the conventional pattern because the ink inside the engraved cell is pushed out by the doctor blade. When electrons are concentrated in a very thin pattern, bottlenecks can occur, which in turn leads to an excessive voltage increase, resulting in a short circuit. This is because the severity of printing defects that can cause a short circuit and the conductance significantly affect the performance of printed electronic devices. However, few studies have been reported on printing defects and conductance with respect to the printing conditions [22].

In this study, we experimentally analyzed the effects of printing conditions, web speed, tension, and nip pressure on drag-out tail defects and conductance. Considering the results, optimal conditions minimizing the drag-out tail defect and conductance were statistically optimized using a Box–Behnken design. Finally, we fabricated two cases of flexible pressure capacitive sensors using the conductive patterns before and after optimization and experimentally verified that the sensor that uses the conductive pattern after the optimization has higher sensitivity than that before the optimization.

2 Factors Affecting the Conductance of the Printed Patterns and Drag-Out Tail Defect

The gravure printing process consists of four phases: inking, doctoring, ink transferring, and ink setting [23, 24]. In the inking phase, ink is deposited on the surface of the gravure printing roll. In the doctoring phase, the ink is filled in the engraved cell, and the ink on the roll surface is wiped out. The ink filled in the engraved pattern is transferred to the web by the nip roll during ink transferring. The transferred ink forms patterns according to the geometric shape of the engraved patterns. The volume of ink transferred to the web can be different according to the properties of the nip roll, such as stiffness, elastic modulus, and nip roll pressure. The printed patterns on the web are widened or agglomerated according to the difference between the surface tension of ink and the surface energy of the substrate in the ink setting. The ink transfer ratio at each phase can be calculated using Eq. (1)

$$\eta_T = \eta_i \cdot \eta_d \cdot \eta_{it} \quad (1)$$

where,

$$\eta_i = \frac{V_{ai}}{V_{bi}}$$

$$\eta_d = \frac{V_{ad}}{V_{ai}}$$

$$\eta_{it} = \frac{V_{it}}{V_{ad}}$$

where η_T denotes the ink transfer ratio; η_i , η_d , and η_{it} denote the ink transfer ratios at the inking, doctoring, and ink transferring phases, respectively; V_{bi} and V_{ai} denote the volumes of the ink filled in the engraved cell before and after the inking, respectively; and V_{ad} and V_{it} denote the volumes of the ink in the engraved cell after doctoring and the volume of the ink transferred to the web, respectively.

Figure 1 presents the schematics of ink transfer in the doctoring and ink transferring. In ink transferring, the tension changes the surface energy of the web and affects the shape of the printed pattern. The web speed could affect V_{it} by changing the shear force of the ink transferred from the engraved cell to the web, as shown in the right-side image in Fig. 1 [25]. V_{it} could also be varied according to the nip pressure by changing the contact area between the ink in the engraved cell and web. Considering that the conductance can be changed according to V_{it} , the tension, web speed, and nip pressure were selected as the factors that affect the conductance. As mentioned earlier, the process variables of gravure

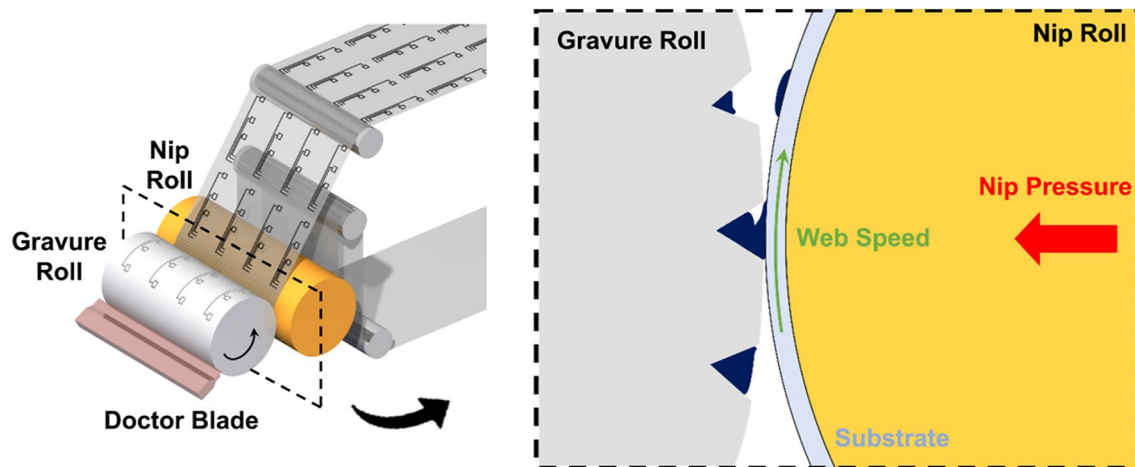


Fig. 1 Relationship of ink transfer mechanism and process condition in gravure printing process

printing affect the ink transfer ratio, which changes the thickness and width of pattern printed on the substrate. In addition, the change in pattern geometry leads to the change in resistance of the printed pattern depending on the process variables, even if the same ink is used [22].

The drag-out tail defect occurs because the fraction of the ink in the engraved cell is adhered under the tip of the doctor blade and drawn out from the cell after doctoring. Figure 2 shows the schematics of the doctoring phase and drag-out tail defects. Figure 2a–c show the behavior of the ink between the tip of the doctor blade and engraved cell (a) before the tip enters the engraved cell, (b) after the tip enters the engraved cell, and (c) after the doctoring, respectively. The doctor blade is fixed, and the gravure roll rotates from left to right as shown in the figure; the tip of the doctor blade leaves the engraved cell relatively. In Fig. 2a, an ink meniscus is formed between the tip and the surface of the roll. After the tip enters the engraved cell, the curvature of the meniscus is increased because the gap between the tip and the ink in the engraved cell increases, as shown in Fig. 2b. After doctoring, the fraction of the ink adhered during doctoring, shown in Fig. 2b, is drawn out to the roll surface, as shown in Fig. 2c. The volume of the drawn ink can be

changed by changing the web speed [21]. If the volume of the drawn ink is excessively large, a drag-out tail defect is generated. The ink volume after doctoring is lower than that before doctoring by the amount of drawn ink. The drag-out tail defect could generate short circuits in multi-line based printed devices. Considering the behavior of ink in the doctoring, we selected the web speed as the factor affecting the severity of the drag-out tail defect.

3 Experiment

We analyzed the effects of the three selected factors on the conductance and drag-out tail defect and statically optimized the factors using the Box–Behnken design. Figure 3 shows (a) the structure of the R2R printing machine, and (b) the gravure printing section. Table 1 summarizes the properties of the polyethylene terephthalate (PET) film (CD-901, KOLON Inc., Korea) and silver ink (TEC-CO-030G, INKTEC Inc., Korea) [26]. We determined the range of the experimental conditions considering the specifications of the gravure printer and ink properties. The maximum web speed was determined by considering the minimum drying time to

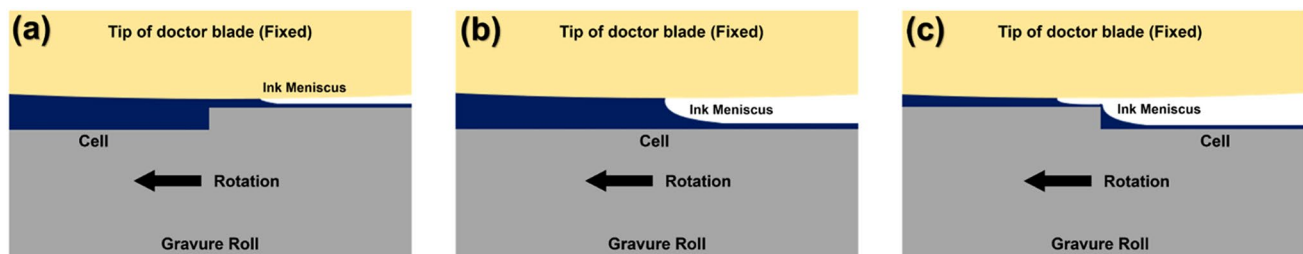


Fig. 2 Doctoring phase: **a** before engraved cell **b** within engraved cell, and **c** after engraved cell

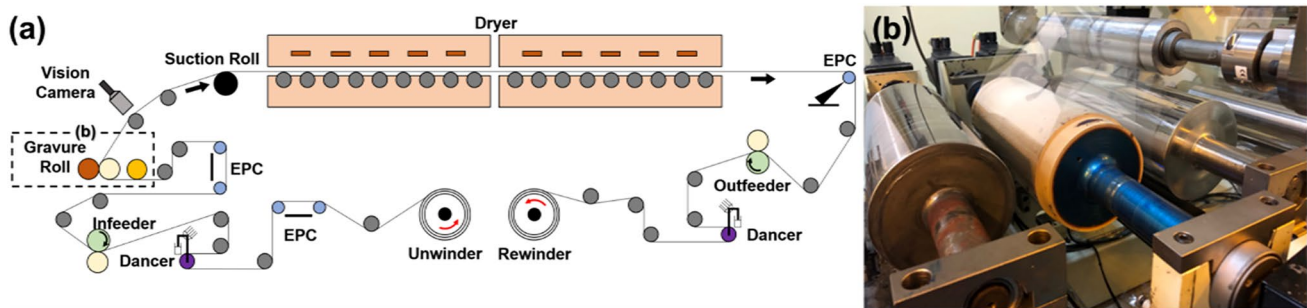


Fig. 3 a Schematic of gravure printing system and b gravure printing unit

Table 1 Mechanical property of the PET film and Ag ink

Material	Property	Unit	Value
PET film	Density	kg/m ³	1390
	Elastic modulus	MPa	5500
	Poisson's ratio	–	0.33
Ag ink	Density	kg/m ³	1400
	Solid content	wt%	20
	Viscosity	cPs	3000

fully evaporate the solvent in the printed pattern. The maximum and minimum web speeds were determined to be 6 and 2 m/min, considering sufficient drying time and the amount of ink which is sufficient for the formation of the printed pattern according to the geometric shape of the engraved pattern transferred to the web in the ink transferring [27]. The range of the tension was set from 2 to 6 kgf considering the minimum tension that can be applied to the web in the machine and 3% of the tensile stress [28]. Considering the minimum nip pressure at which the sufficient ink is transferred to the substrate during ink transfer, we determined the range of the nip pressure from 0.4 to 0.55 MPa, and the maximum nip pressure in the R2R machine. Considering the poor doctoring quality at low doctoring pressure, we fixed the doctoring pressure to 0.6 MPa. The drying temperature was set to 150 °C considering the curing temperature of the

ink according to the drying time, determined by the length of the dryer and the maximum web speed in this experiment [29, 30]. Figure 4 presents the images of the ink particle at (a) room temperature and (b) cured at 150 °C, respectively. Table 2 indicates the experimental order determined by the Box–Behnken design and the corresponding resistance and severity of the drag-out tail defect. The Box–Behnken design is generally used to statistically optimize the input conditions. This method has a smaller number of experiments and is safer than central composite design [27]. Figure 5 shows (a) the printed conductive pattern, (b) the resistance measurement line of length 54.4 mm and the region where the drag-out tail was measured in the same pattern. The representative value of the pattern resistance was measured as follows. The resistance of each of the 12 samples printed under same process conditions was measured, and the average value excluding the maximum and minimum values was taken. The severity of drag-out tail was evaluated by the average length of the drag-out tail. The images of the patterns were captured using a microscope (LV100ND, Nikon, Japan). The lengths of drag-out tail were measured at each point by dividing the distance from the end of the pattern to a point 500 μm away into 10 equal parts. We measured the length of drag-out tail by referring to the study in Subramanian et al. [21]. Figure 6 shows the conductive pattern images for (a) case 1, (b) 5, (c) 6, and (d) 10, and the corresponding severity of the drag-out tail. Remaining cases in between 1

Fig. 4 Surface scanning electron microscopy (SEM) image of printed pattern dried at a room temperature and b 150 °C

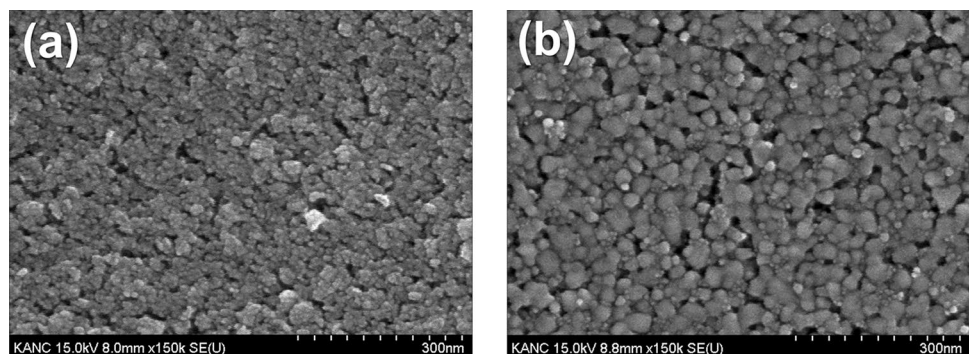
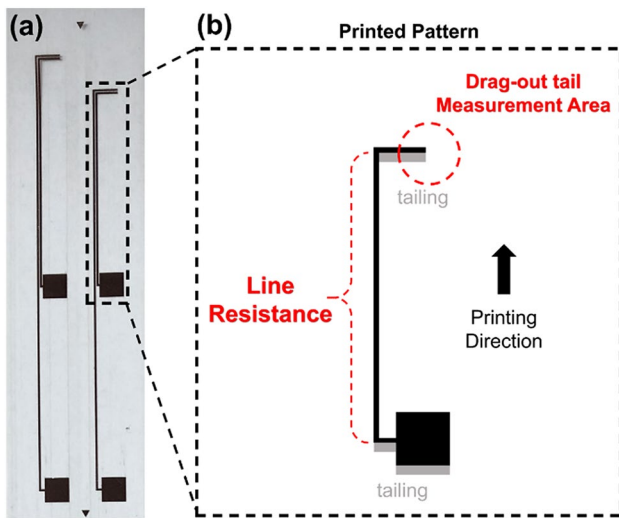


Table 2 Resistance and drag-out tail length of conductive layer because of experimental case

Case	Web tension (kgf)	Web speed (mpm)	Nip pressure (MPa)	Resistance (Std.) (Ω)	Drag-out tail (μm)
1	2	2	0.475	41.43 (0.15)	107.78
2	2	4	0.4	39.83 (0.16)	75.25
3	2	4	0.55	38.17 (0.16)	78.64
4	2	6	0.475	40.33 (0.21)	51.15
5	4	2	0.4	40.3 (0.08)	102.3
6	4	2	0.55	38.73 (0.14)	118.8
7	4	4	0.475	38.73 (0.13)	89.70
8	4	6	0.4	39.8 (0.14)	73.49
9	4	6	0.55	36.2 (0.04)	119.1
10	6	2	0.475	36.87 (0.16)	121.6
11	6	4	0.4	38.63 (0.15)	81.27
12	6	4	0.55	34.43 (0.11)	85.21
13	6	6	0.475	36.4 (0.13)	66.27

**Fig. 5** a Conductive layer pattern manufactured through gravure printing process, b measurement section of line resistance and c measurement area of drag-out tail defect

to 13 has been sorted as supplementary data by Figure S1. Figure 7 shows the main effects and interaction effects of the factors affecting the resistance of the printed patterns. One can observe that the resistance decreases with increasing web speed, tension, and nip pressure.

The surface roughness of the web decreases with increasing tension; accordingly, the surface energy of the web is increased. The ink transferred to the web is more widened after the ink transfer, and the printed pattern is more uniform, which could decrease the resistance [31, 32]. The increase in the web speed could increase the shear force generated in the ink between the engraved cell and the web during ink transfer. If the shear force is increased, more ink is transferred to the web; accordingly, the pattern resistance

is decreased [18]. Figure 8 presents the forces applied at the ink in the engraved cell and (b) the conceptual figure of the behavior of the web by the increase in the nip pressure in the ink transferring. In Fig. 8a, F_{IS} , F_{IC} , and F_I are the adhesive forces between the inks, the ink and engraved cell, and cohesive force in the ink, respectively. The ink transfer ratio increased with increasing F_{IS} and F_I . If F_{IS} and F_I are larger than F_{IC} , the ink filled in the engraved cell is completely transferred to the web [22]. F_{IS} is proportional to the product of the work of adhesive forces at the interface between the ink and web (W_{IS}) and the contact length between the web and ink (L_{IS}) [15]. If the nip pressure increases, L_{IS} is increased, as shown in Fig. 8b; accordingly, the ink transfer ratio is also increased.

Figure 9 shows the main effects and interaction effects of the factors on drag-out tail. As shown, drag-out tail increases with increasing tension and nip pressure and decreasing web speed. As mentioned above, the ink transfer ratio in the ink transferring increased with increasing nip pressure. The printed pattern is more widened with higher tension. The increase in the nip pressure could also increase the transfer ratio of the ink forming the drag-out tail. Moreover, the transferred drag-out tail defect could widen in the higher tension. If the web speed is increased, the amount of drawn ink from the engraved cell in the doctoring is decreased, and therefore, the drag-out tail is decreased [21].

4 Optimization of Conductive Layer Considering Resistance and Drag-Out Tail Defect

Considering the experimental results shown in Sect. 3, we derived the optimal conditions of the factors. The desirability function was used to numerically evaluate the printed

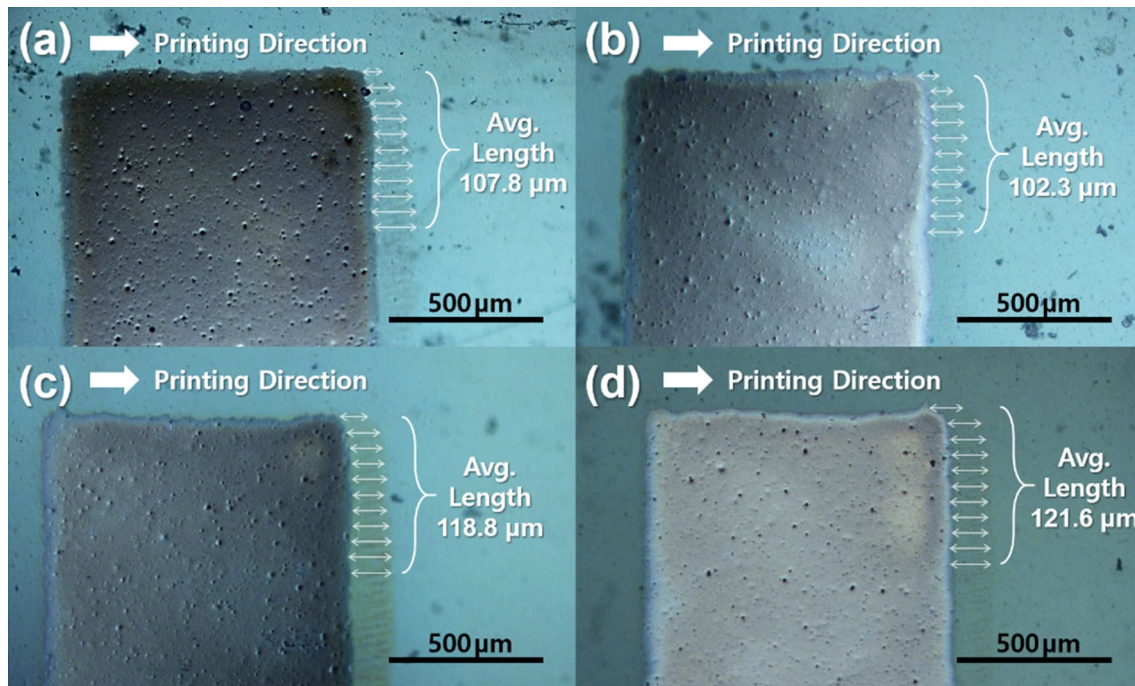


Fig. 6 Length of drag out tail in **a** case 1, **b** case 5, **c** case 6, and **d** case 10

pattern quality considering the resistance and drag-out tail according to the factors. Equation (3) presents the desirability function used in the optimization [33, 34] as follows:

$$d_m = \begin{cases} 0 & \text{if } y < T \\ \left(\frac{y-M}{T-M}\right)^s & \text{if } T \leq y \leq M \\ 1 & \text{if } y > M \end{cases} \quad (3)$$

where d_m denotes the desirability value; y the measured output value; T and M the target value and the permissible maximum value set by a user, respectively; and s the weight factor. We set s as 0.5

The overall desirability was calculated as the geometric mean of the desirability values of the resistance and drag-out tail, as shown in the following Eq. (4) [35]:

$$d_{m,\text{total}} = \sqrt{d_{m,r} \cdot d_{m,t}} \quad (4)$$

where $d_{m,\text{total}}$ denotes the overall desirability, and $d_{m,r}$ and $d_{m,t}$ denote the desirability values of the resistance and drag-out tail, respectively.

Using Eqs. (3) and (4), we obtained the optimal values of the web speed, tension, and nip pressure as 6 m/min, 6 kgf, and 0.5235 MPa, respectively. Figure 10 presents the overall desirability of all experimental cases in Table 3 and the optimal conditions. The number below each overall desirability is its experimental number, as shown in Table 3. The red and

blue boxes represent the ideal desirability 1 and the overall desirability of the patterns printed in the optimal conditions, which is 0.8295. Figure 11 shows the conductive pattern obtained under the optimal conditions. The resistance and the drag-out tail severity were 30.87 Ω and 74.37 μm , respectively. The resistance and the drag-out tail severity were improved by 74% and 53%, respectively, compared with the conductive pattern printed in the conventional case.

5 Application: Capacitive Pressure Sensor

We fabricated two pressure capacitive sensors using conductive patterns before and after optimization. Figure 12 presents (a) the schematics of the pressure capacitive sensor and (b) the fabricated sensor. The geometry of the measurement section was 6*6 mm. Barium titanate (BaTiO_3) was used as the dielectric layer of the sensor, which was coated using slot-die coating process. Table 3 summarizes the properties of the dielectric ink.

Figure 13 presents (a) the ratio of capacitance between the capacitance values at each load and at the initial load conditions, and (b) their sensitivity. One can observe that the sensitivity of the sensor using the conductive pattern after the optimization is higher than that before the optimization at 0–35 kgf of load. In particular, the sensitivity of the sensor after optimization is much higher than before

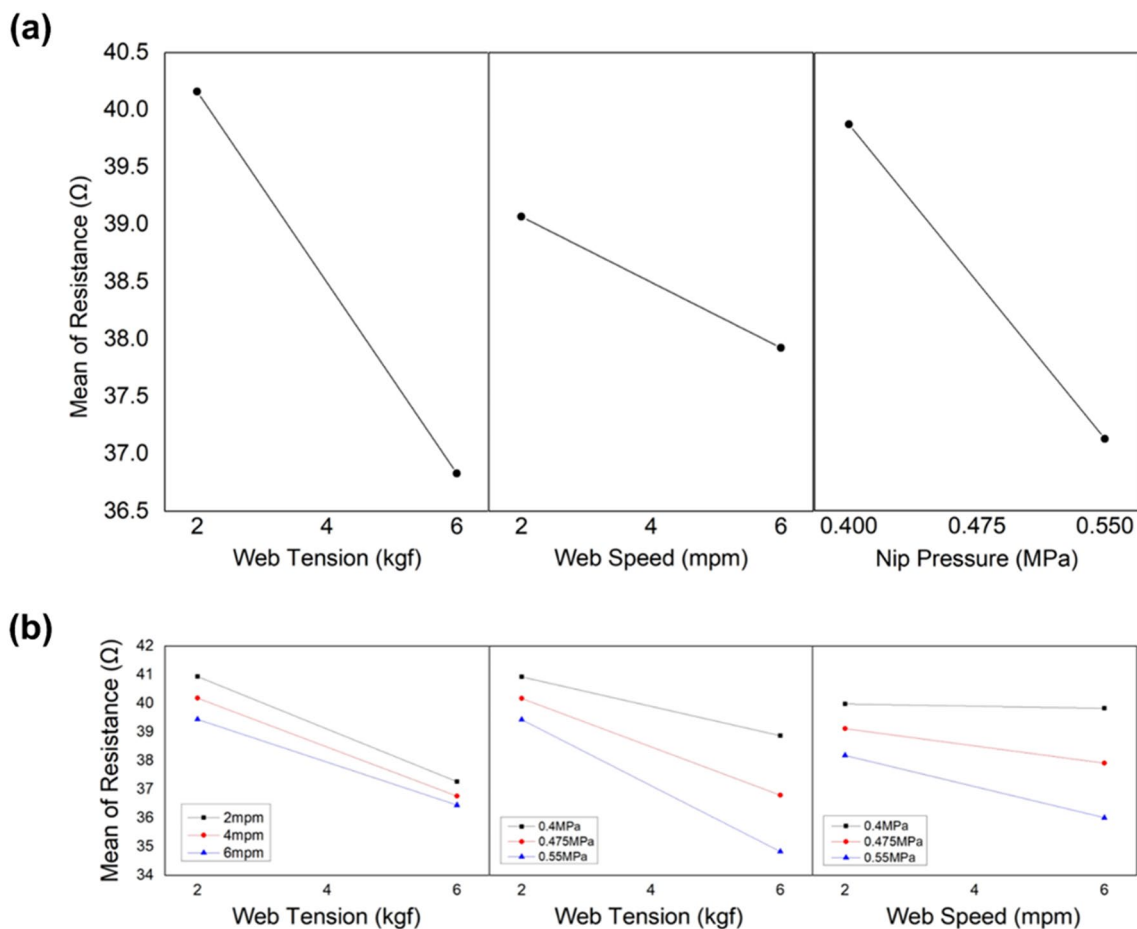
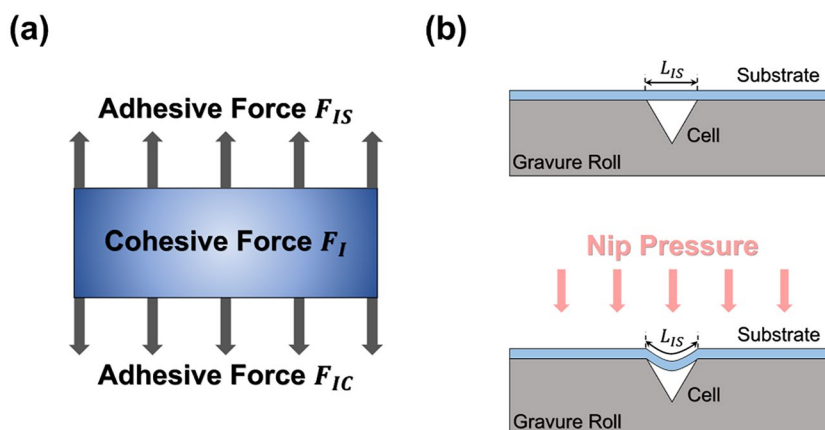


Fig. 7 Main effects and interaction plots for resistance according to process variables

Fig. 8 a Three forces applied to ink in an engraved cell and b change of contact length under nip pressure



optimization in 0–10 kgf of load. When the resistance of the conductive layer decreases, more electrons with less energy loss can accumulate on the capacitor plate. As a result, the polarization of the dielectric layer becomes

more active, which increases the capacitance. The maximum capacitance of a capacitor manufactured based on the conductive layer before improvement is 187.01 pF and that after improvement is 442.5 pF. Thus, the capacitance

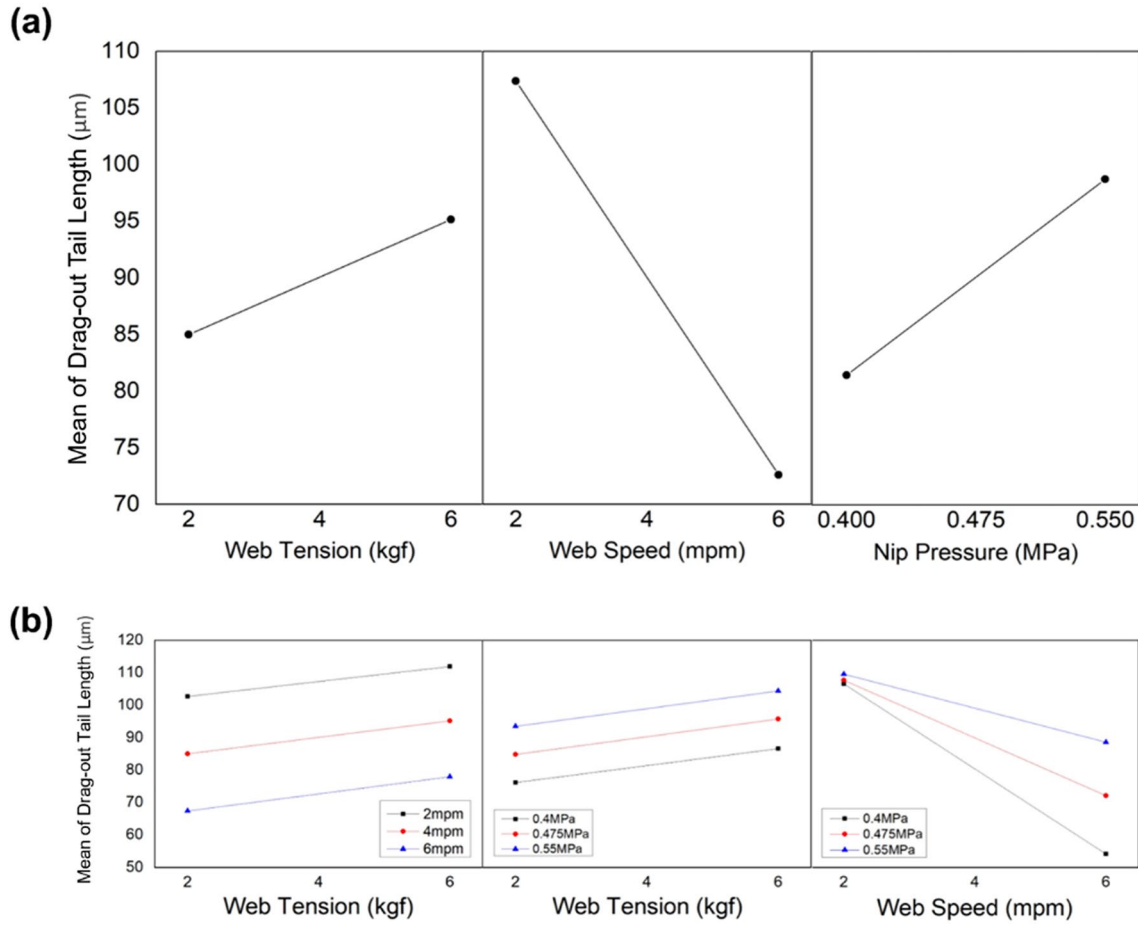


Fig. 9 Main effects and interaction plots for drag-out tail according to process variables

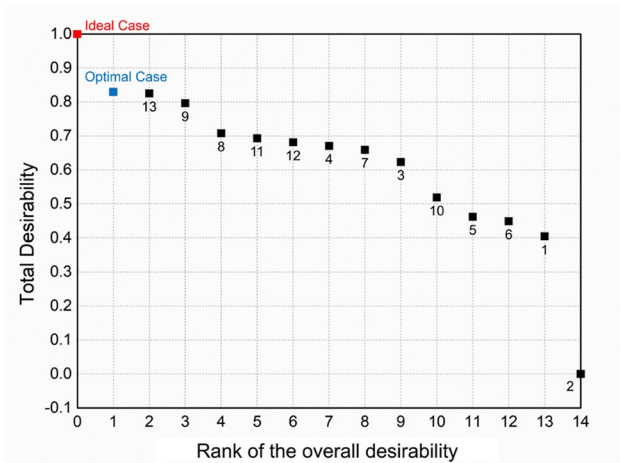


Fig. 10 Overall desirability of printed electronic patterns

Table 3 Material properties of dielectric ink

Property	Unit	Value
Viscosity	cPs	80
Solid contents	wt%	40
Surface tension	mN/m	32
Relative dielectric constant	–	20

increased by about 236%. Further, the maximum sensitivity of the capacitor before and after improvement were 0.21 and 0.41, respectively, which suggests an improvement of about 195%. Moreover, the average sensitivities before and after the improvement was 0.021 and 0.041, respectively. The results clearly show that the sensor using the conductive pattern after the optimization has a much higher sensitivity than that before optimization.

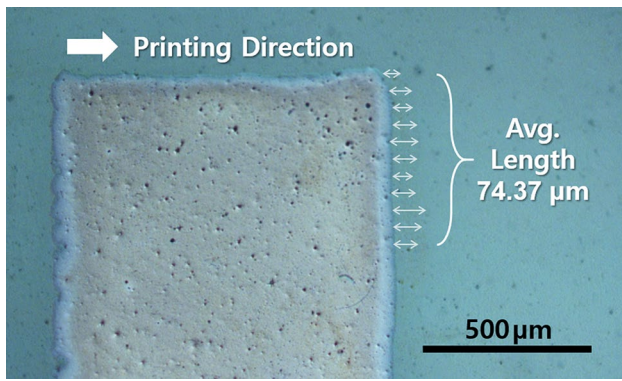


Fig. 11 Microscopic view of electronic pattern printed under the optimal condition

6 Conclusion

Herein, the effects of the printing conditions, web speed, tension, and nip pressure on the drag-out tail defect and conductance were analyzed. It can be observed that the resistance decreases with increasing web speed, tension, and nip pressure. The drag-out tail increases with increasing tension and nip pressure and decreasing web speed. Considering these results, optimal conditions minimizing the drag-out tail defect and conductance were optimized using the Box–Behnken design. Under the optimal conditions, the resistance and drag-out tail severity are improved by 74% and 53%, respectively, compared with the conductive pattern printed in the conventional case. Finally, we fabricated two cases of flexible pressure capacitive sensors using the conductive patterns before and after the optimization, and experimentally verified that the sensor using the conductive pattern after the optimization has higher sensitivity than before the optimization.

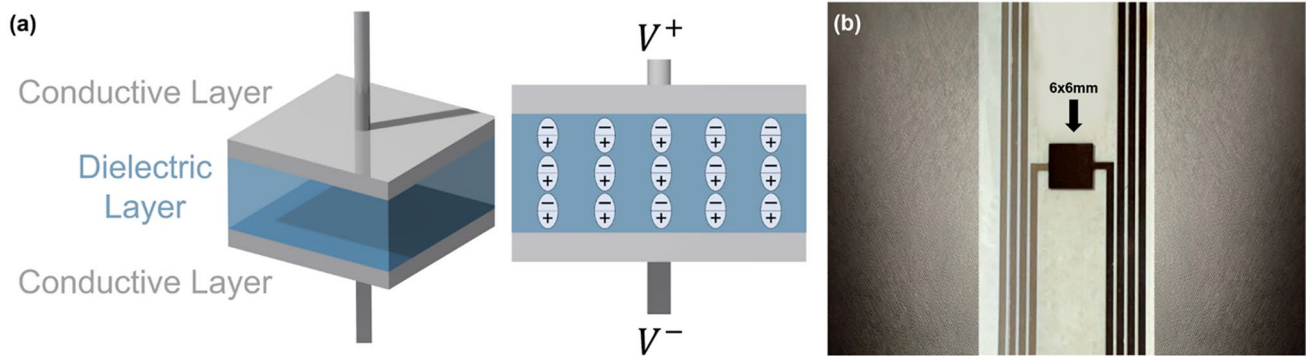


Fig. 12 **a** Structure of the pressure sensitive capacitor and **b** fabricated sensor

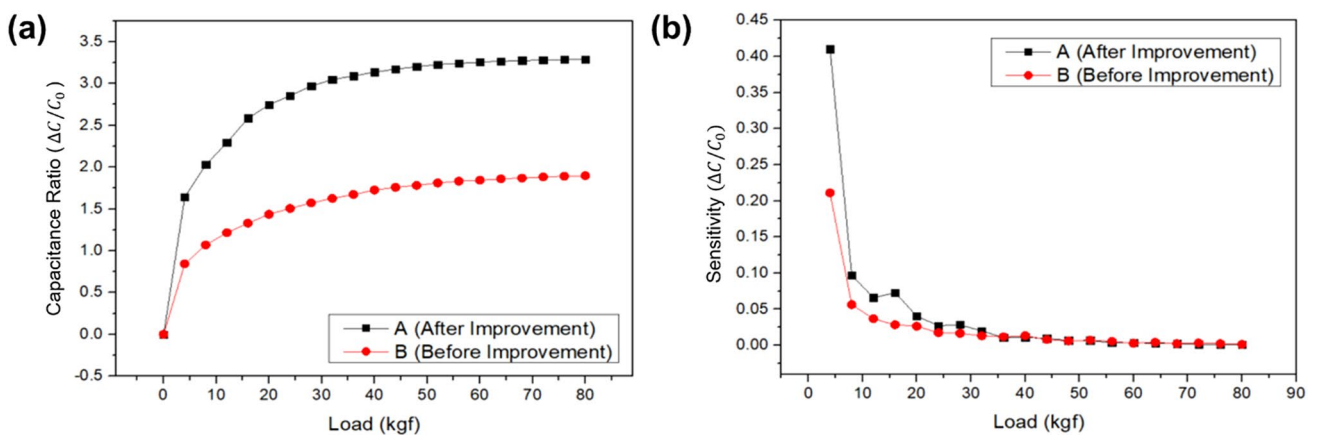


Fig. 13 **a** Capacitance ratio and **b** capacitance variation under increasing load conditions

Supplementary Information The online version contains supplementary material available at <https://doi.org/10.1007/s40684-021-00345-4>.

Acknowledgements This work was supported by a National Research Foundation of Korea (NRF) grant funded by the Korea Government (MIST) (No. 2020R1A2C1012428) & (No. 2020R1A5A1019649).

Funding This work was supported by a National Research Foundation of Korea (NRF) grant funded by the Korea Government (MIST) (No. 2020R1A2C1012428) & (No. 2020R1A5A1019649).

Declarations

Conflict of interest This manuscript has not been published or presented elsewhere in part or in entirety and is not under consideration by another journal. We have read and understood your journal's policies, and we believe that neither the manuscript nor the study violates any of these. There are no conflicts of interest to declare.

References

- Choi, H., & Jeong, S. (2018). A review on eco-friendly quantum dot solar cells: Materials and manufacturing processes. *International Journal of Precision Engineering and Manufacturing-Green Technology*, 5(2), 349–358.
- Lee, Y. H., Chang, I., Cho, G. Y., Park, J., Yu, W., Tanveer, W. H., & Cha, S. W. (2018). Thin film solid oxide fuel cells operating below 600 C: A review. *International Journal of Precision Engineering and Manufacturing-Green Technology*, 5(3), 441–453.
- Wang, S., Huang, K. H., & Yang, Y. J. (2019). A Highly Sensitive Capacitive Pressure Sensor with Microdome Structure for Robot Tactile Detection. In *2019 20th International Conference on Solid-State Sensors, Actuators and Microsystems & Eurosensors XXXIII (TRANSDUCERS & EUROSENSORS XXXIII)* (pp. 458–461). IEEE.
- Fastier-Wooller, J., Dinh, T., Dau, V. T., Phan, H. P., Yang, F., & Dao, D. V. (2018). Low-cost graphite on paper pressure sensor for a robot gripper with a trivial fabrication process. *Sensors*, 18(10), 3300.
- Pfeifer, R., Lungarella, M., & Iida, F. (2012). The challenges ahead for bio-inspired 'soft' robotics. *Communications of the ACM*, 55(11), 76–87.
- Zhu, Y., Li, J., Cai, H., Wu, Y., Ding, H., Pan, N., & Wang, X. (2018). Highly sensitive and skin-like pressure sensor based on asymmetric double-layered structures of reduced graphite oxide. *Sensors and Actuators B: Chemical*, 255, 1262–1267.
- Chen, D., & Pei, Q. (2017). Electronic muscles and skins: a review of soft sensors and actuators. *Chemical Reviews*, 117(17), 11239–11268.
- Zang, Y., Zhang, F., Di, C. A., & Zhu, D. (2015). Advances of flexible pressure sensors toward artificial intelligence and health care applications. *Materials Horizons*, 2(2), 140–156.
- Ai, Y., Hsu, T. H., Wu, D. C., Lee, L., Chen, J. H., Chen, Y. Z., & Chueh, Y. L. (2018). An ultrasensitive flexible pressure sensor for multimodal wearable electronic skins based on large-scale polystyrene ball@ reduced graphene-oxide core-shell nanoparticles. *Journal of Materials Chemistry C*, 6(20), 5514–5520.
- Kim, K. H., Hong, S. K., Jang, N. S., Ha, S. H., Lee, H. W., & Kim, J. M. (2017). Wearable resistive pressure sensor based on highly flexible carbon composite conductors with irregular surface morphology. *ACS Applied Materials & Interfaces*, 9(20), 17499–17507.
- Zhuo, B., Chen, S., Zhao, M., & Guo, X. (2017). High sensitivity flexible capacitive pressure sensor using polydimethylsiloxane elastomer dielectric layer micro-structured by 3-D printed mold. *IEEE Journal of the Electron Devices Society*, 5(3), 219–223.
- Shi, J., Wang, L., Dai, Z., Zhao, L., Du, M., Li, H., & Fang, Y. (2018). Multiscale hierarchical design of a flexible piezoresistive pressure sensor with high sensitivity and wide linearity range. *Small (Weinheim an der Bergstrasse, Germany)*, 14(27), 1800819.
- Wang, R., Kwon, H. J., Tang, X., Ye, H., Park, C. E., Kim, J., & Kim, S. H. (2020). Slot-die coating of sol-gel-based organic-inorganic nanohybrid dielectric layers for flexible and large-area organic thin film transistors. *Applied Surface Science*, 529, 147198.
- Noh, J., Yeom, D., Lim, C., Cha, H., Han, J., Kim, J., & Cho, G. (2010). Scalability of roll-to-roll gravure-printed electrodes on plastic foils. *IEEE Transactions on Electronics Packaging Manufacturing*, 33(4), 275–283.
- Nguyen, H. A. D., Shin, K., & Lee, C. (2015). Effect of nip force on ink transfer in high resolution roll-to-roll printing. *International Journal of Precision Engineering and Manufacturing*, 16(3), 517–523.
- Shin, K. H., Nguyen, H. A. D., Park, J., Shin, D., & Lee, D. (2017). Roll-to-roll gravure printing of thick-film silver electrode micropatterns for flexible printed circuit board. *Journal of Coatings Technology and Research*, 14(1), 95–106.
- Lee, C., & Shin, K. H. (2013). A mathematical model to predict surface roughness and pattern thickness in roll-to-roll gravure printed electronics. *Robotics and Computer-Integrated Manufacturing*, 29(4), 26–32.
- Lee, T. M., Lee, S. H., Noh, J. H., Kim, D. S., & Chun, S. (2010). The effect of shear force on ink transfer in gravure offset printing. *Journal of Micromechanics and Microengineering*, 20(12), 125026.
- Lee, C., Kang, H., Kim, C., & Shin, K. (2010). A novel method to guarantee the specified thickness and surface roughness of the roll-to-roll printed patterns using the tension of a moving substrate. *Journal of Microelectromechanical Systems*, 19(5), 1243–1253.
- Kang, H., & Lee, C. (2015). Effect of tension on conductivity of gravure printed ag layer in roll-to-roll process. *International Journal of Precision Engineering and Manufacturing*, 16(1), 99–104.
- Kitsomboonloha, R., Morris, S. J. S., Rong, X., & Subramanian, V. (2012). Femtoliter-scale patterning by high-speed, highly scaled inverse gravure printing. *Langmuir*, 28(48), 16711–16723.
- Nguyen, H. A. D., Lee, C., Shin, K. H., & Lee, D. (2015). An investigation of the ink-transfer mechanism during the printing phase of high-resolution roll-to-roll gravure printing. *IEEE Transactions on Components, Packaging and Manufacturing Technology*, 5(10), 1516–1524.
- Lee, S., & Na, Y. (2010). Analysis on the ink transfer mechanism in R2R application. *Journal of Mechanical Science and Technology*, 24(1), 293–296.
- Nguyen, H. A. D., Lee, J., Kim, C. H., Shin, K. H., & Lee, D. (2013). An approach for controlling printed line-width in high resolution roll-to-roll gravure printing. *Journal of Micromechanics and Microengineering*, 23(9), 095010.
- Kim, S., Lee, J., Jo, M., & Lee, C. (2020). Numerical modeling of ink widening and coating gap in roll-to-roll slot-die coating of solid oxide fuel cell electrolytic layer. *Polymers*, 12(12), 2927.
- Nikitin, P. V., Lam, S., & Rao, K. V. S. (2005). Low cost silver ink RFID tag antennas. In *2005 IEEE Antennas and Propagation Society International Symposium* (Vol. 2, pp. 353–356). IEEE.
- Lee, J., Park, J., Jeong, H., Shin, K. H., & Lee, D. (2016). Optimization of printing conditions for microscale multiline printing

- in continuous roll-to-roll gravure printing. *Journal of Industrial and Engineering Chemistry*, 42, 131–141.
28. Hawkins, W. E. (2002). *Web Stability. The plastic film and foil web handling guide* (pp.3–19). Boca Raton: CRC Press.
 29. Lee, J., Byeon, J., & Lee, C. (2020). Fabrication of Thickness-Controllable Double Layer Electrolyte Using Roll-to-Roll Additive Manufacturing System. *International Journal of Precision Engineering and Manufacturing-Green Technology*, 1–8.
 30. Jo, M., Lee, J., Kim, S., Cho, G., Lee, T. M., & Lee, C. (2020). Web unevenness due to thermal deformation in the roll-to-roll manufacturing process. *Applied Sciences*, 10(23), 8636.
 31. Lee, J., Byeon, J., & Lee, C. (2020). Theories and Control Technologies for Web Handling in the Roll-to-Roll Manufacturing Process. *International Journal of Precision Engineering and Manufacturing-Green Technology*, 1–20.
 32. Park, J., Kim, S., & Lee, C. (2018). An analysis of pinned edge layer of slot-die coated film in roll-to-roll green manufacturing system. *International Journal of Precision Engineering and Manufacturing-Green Technology*, 5(2), 247–254.
 33. Candiotti, L. V., De Zan, M. M., Cámara, M. S., & Goicoechea, H. C. (2014). Experimental design and multiple response optimization. Using the desirability function in analytical methods development. *Talanta*, 124, 123–138.
 34. Kim, S., Lee, J., & Lee, C. (2019). Computational fluid dynamics model for thickness and uniformity prediction of coating layer in slot-die process. *The International Journal of Advanced Manufacturing Technology*, 104(5–8), 2991–2997.
 35. Yeo, L. P., Yan, Y. H., Lam, Y. C., & Chan-Park, M. B. (2006). Design of experiment for optimization of plasma-polymerized octafluorocyclobutane coating on very high aspect ratio silicon molds. *Langmuir*, 22(24), 10196–10203.

Publisher's Note Springer Nature remains neutral with regard to jurisdictional claims in published maps and institutional affiliations.



Minho Jo received the B.Eng. degree in the Department of Mechanical Engineering, from Konkuk University, Seoul, Korea, in 2020, and he is currently working toward the M.Eng. degree with the Department of Mechanical Design and Production Engineering in Konkuk university, Seoul, Korea. He has studied the web handling in the Roll-to-Roll printed electronics, dynamics of flexible substrate in drying process, and taper tension control in winding process. His research

interests included web handling, dynamics of lateral motion and tension control in Roll-to-Roll systems.



Jongsu Lee received the B.Eng., M.Eng., and Ph.D degrees in the Department of Mechanical Design and Production Engineering from Konkuk University, Seoul, South Korea, in 2011, 2013, and 2019, respectively. He was with the laboratory of Polymer Innovation for Advanced Organic Electronics at Purdue University as a postdoctoral research fellow. He is currently an assistant professor at Department of Printed Electronics Engineering, Suncheon National University, South Korea. He has

studied the dynamics of flexible films including those of composite ones in large-scale systems such as steel plant, film and paper making plant, and roll-to-roll printing system, fabrication of printed functional devices, theoretical and statistical optimization of the systems, fault diagnosis, and tension and register control. His research interests include design of large-scale web handling systems, printed electronics, tension and register control, and fault diagnosis.



Seongyong Kim received the B.Eng. and M.Eng. degrees from the Department of Mechanical Design Engineering, Changwon National University, in 2014, 2016, respectively. He is currently working toward the Ph.D degree with the Department of Mechanical Design and Production Engineering. He has studied the radial stress distribution of winding system, computational fluid dynamics of slot-die coating process and dynamics of the flexible substrate in lamination process. His research interest

includes printed electronic, CFD and FEM analysis in the roll-to-roll process including slot-die coating.



Gyoujin Cho received the Ph.D. degree Oklahoma, Norman, OK, USA, in 1995. From 1996 to 2008, he was with the Department of Chemical Engineering, Suncheon National University, South Korea, as a Professor of Printed Electronics Engineering, World Class University (WCU) Program, Suncheon National University. Since 2019, he has been a Professor with the Department of Biophysics, Sungkyunkwan University. With special expertise in printed electronics engineering, Prof.

Cho has worked on leading fully R2R printed wireless sensors, limitless TFT-active matrix-based signage, and biosensors. He has also served as an Editor of *Printing Technologies in Flexible and Printed Electronics*, IOP Science, since 2016.



Taik-Min Lee received the B.S. degree in the Department of Precision Engineering from Korea Advanced Institute of Science and Technology (KAIST), Daejeon, South Korea, in 1995, and M.S., and Ph.D degrees in the Department of Mechanical Engineering from Korea Advanced Institute of Science and Technology (KAIST), Daejeon, South Korea, in 1997, 2002 respectively. He is currently a principal researcher with the Intelligence and Precision Machinery Research Division, Korea Institute of Machinery & Materials (KIMM), South Korea. His research interests lie in the fields of the printing process and equipment development for electronic devices, display parts, sensors, and such as OLED, flexible display, roll to roll battery, solar cell, and quantum biosensor. He has abundant experience to make a draft for a technical white paper since he has been working for the government to launch a new research program. Nowadays, he is collaborating with quantum experts for launching quantum biosensor research program in Korea.

of Machinery & Materials (KIMM), South Korea. His research interests lie in the fields of the printing process and equipment development for electronic devices, display parts, sensors, and such as OLED, flexible display, roll to roll battery, solar cell, and quantum biosensor. He has abundant experience to make a draft for a technical white paper since he has been working for the government to launch a new research program. Nowadays, he is collaborating with quantum experts for launching quantum biosensor research program in Korea.



Changwoo Lee received the B.Eng, M.Eng. and Ph.D. degrees in the Department of Mechanical Engineering from Konkuk University, Seoul, South Korea, in 2001, 2003, and 2008, respectively. From 2013 to 2018, he was an associate professor at Department of Mechanical Engineering, Changwon National University. He is currently an associate professor at Department of Mechanical Engineering, Konkuk University. His research interests lie in the fields of web handling system, fault

diagnosis, fault-tolerant control, roll-to-roll printing and coating system, non-contacting transportation, tension and register control, finite element analysis of the flexible films in large-scale systems. He was awarded the 2017 KSPE's Baek-Am Paper Award that honors the author of the best paper presented in the Journal of KSPE for the last three years.